

# Migration Velocity of Cell under Shear Flow Field: After and Before Division

Shigehiro Hashimoto, *Member IEEE*  
dept. Mechanical Engineering  
Kogakuin University  
Tokyo, Japan  
shashimoto@cc.kogakuin.ac.jp

Kiyoshi Yoshinaka  
Health and Medical Research Institute  
National Institute of Advanced Industrial Science & Technology  
Tsukuba, Japan  
k.yoshinaka@aist.go.jp

**Abstract**— The migration velocity of each single cell under the Couette type of the shear flow field has been studied in relation to the area adhere to the scaffold before and after division *in vitro*. The shear field was made in a constant gap between a lower stationary culture plate and an upper rotating parallel plate. Two types of cells were used in the test: L929 (mouse fibroblast connective tissue), and 3T3-L1 (mouse fat precursor cells). After adhesion of cells on the lower plate, the wall shear stress of 1 Pa was continuously applied on cells for 24 hours in an incubator. The migration velocity of each cell was traced at the time lapse images observed by an inverted phase contrast microscope placed in an incubator. Experimental results show that the migration of each cell is accelerated with the smaller contact area between the cell and the scaffold around the term of division of the cell. Several cells of L929 migrate to the direction perpendicular to the flow just before division. Although many cells migrate upstream, 3T3-L1 tends to migrate downstream.

**Keywords**— *biomedical engineering, shear stress, division, migration, L929, 3T3-L1, Couette flow*

## I. INTRODUCTION

Biological cells perform various activities on the scaffold: migration, deformation, proliferation, orientation, and differentiation. These activities of each cell lead to the tissue formation through interaction between cells. Each tissue has its own cell arrangement. The control methodology can be applied to the innovative technology for the engineered tissue formation.

Cells receive various forces, sense the forces, and respond to the forces *in vivo*. The uniform mechanical force field around the whole cell can be realized easier with the fluid than with the solid. The shear flow field of the medium has been used to apply the force field to cells [1]. Endothelial cells, for example, are exposed to a shear fluid field of the blood flow, and align to the flow direction on the inner surface of the vessel wall. The effects of the shear flow on the endothelial cells were investigated in many studies [2–6]. Myoblasts, on the other hand, align perpendicular to the flow. In the previous study with the vortex flow by the swinging plate *in vitro*, C2C12 made orientation perpendicular to the direction of the flow, although HUVEC made orientation along the streamline of the flow [7].

The interaction between cells governs the activity of each cell. The alignment of each cell depends on that of adjacent cells [8]. In the basic present study, cells have been sparsely cultured, and the activity of each single cell has been traced. The orientation of each cell affects the orientation of cells in subsequently formed tissues. Cell movement is not only passive, but also active. The direction of active migration can be associated with subsequent cell activity.

In several cases, cells are exposed to the shear stress both *in vivo* and *in vitro*. The direction of the shear stress field might affect the direction of the migration of the cell [1]. The effect might be maintained as the memory in the cell. The hysteresis also can affect the direction of the migration [9]. The behavior of each cell might depend on the initial state. In the most of tests *in vitro*, cells are incubated for several hours for adhesion to the scaffold before the flow stimulation. Each cell, on the other hand, can make division under the wall shear stress field [8]. Is the effect maintained in each cell after division? The adhesion status of the cell is controlled by itself after division. In the present study, the timing of division has been used for the natural initial state for the test exposure to the force field. The migration of each cell has been traced after the division in the shear stress field of the medium in the present study.

At the wall shear stress, a cell might show the following responses: elongation [4], tilting to the streamline [7], migration [5, 10], deformation to be rounded [10], proliferation [6], and exfoliation from the wall of the scaffold [11]. The mild wall shear stress of 1 Pa has been applied in the present study to observe migration of cells during the cell culture *in vitro*.

In the Hagen-Poiseuille type of flow, the shear rate depends on the distance from the wall: highest at the wall. In the Couette type of flow, on the other hand, the shear rate is constant regardless of the distance from the wall [2, 12]. In the present study, A parallel disk type of device for Couette flow in the constant gap between a rotating disk and a stationary dish has been designed to apply the shear stress quantitatively on the cell during incubation at the microscopic observation *in vitro*. The migration velocity of each single cell under the Couette type of the shear flow field has been studied in relation to the area adhere to the scaffold before and after division *in vitro*.

## II. METHODS

### A. Parallel Disk Type of Device for Couette Flow

A parallel disk type of device for Couette flow has been used: between a rotating disk and a stationary dish (Fig. 1). The medium is sheared between a rotating wall and a stationary wall. The stationary wall is the bottom of the culture dish of 60 mm diameter.

In the device, the shear rate ( $\gamma$ ) in the medium is calculated by (1).

$$\gamma = r \omega / d \quad (1)$$

In (1),  $\omega$  is the angular velocity, and  $d$  is the distance between a rotating wall and a stationary wall. Between two

parallel walls,  $d$  is constant. The shear rate ( $\dot{\gamma}$ ) in the gap between two walls increases in proportion to the distance ( $r$ ) from the rotating axis (1).

The angular velocity  $\omega$  smaller than  $22 \text{ rad s}^{-1}$  was controlled by the stepping motor. The value of  $r$  varies between 17 mm and 18 mm in the observation area of the microscope. The distance  $d$  was around 0.6 mm, which was measured by the positions of the walls at the focus of the objective lens of the microscope. Each wall surface position of the gap can be detected by focusing at the microscope. The focusing point can be reproduced by the memory of the position of the focus adjusting ring of the microscope. The shear rates ( $\dot{\gamma}$ ) of  $6.7 \times 10^2 \text{ s}^{-1}$  are made in the present experiment by adjustment of these parameters.

The shear stress ( $\tau$ ) is calculated by the viscosity ( $\eta$ ) of the medium.

$$\tau = \eta \dot{\gamma} \quad (2)$$

The viscosity of the medium of  $1.5 \times 10^{-3} \text{ Pa s}$  was measured by a cone and plate viscometer at 310 K. The shear stress  $\tau$  has been calculated as the value of 1 Pa.

The parallel disk type of device was mounted on the stage of the inverted phase contrast microscope. The microscope with the device was placed in the incubator. The experimental system allows the microscopic observation of cells cultured on the stationary wall during exposure to the shear flow.

### B. Cell Types

Two types of cells were used in the test: L929 (fibroblast connective tissue of C3H mouse), and 3T3-L1 (mouse fat precursor cells, a cell line derived from cells of mouse 3T3). Cells were cultured in D-MEM (Dulbecco's Modified Eagle's Medium): containing 10% decomplexed FBS (fetal bovine serum), and 1% penicillin/ streptomycin.

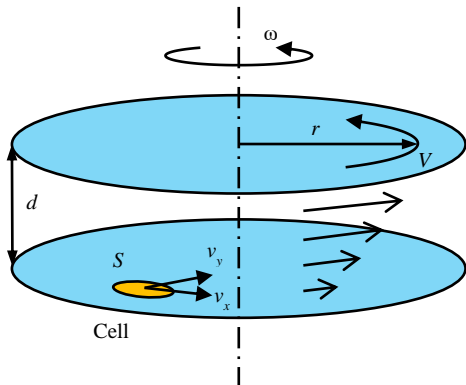


Fig. 1. Couette flow (velocity ( $V$ ) distribution) between rotating (angular velocity  $\omega$ ) wall and stationary wall at  $r$  (radius) with distance  $d$ : migration velocity ( $v_x, v_y$ ) of cell on stationary wall.

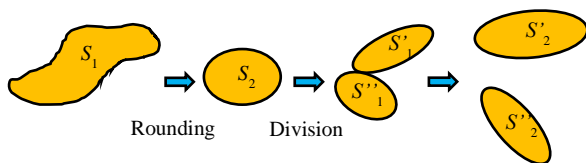


Fig. 2. Area ( $S$ ) change of cell before and after division.

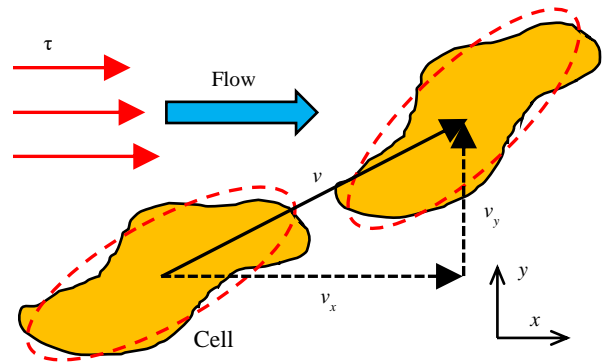


Fig. 3. Migration velocity ( $v_x, v_y$ ) of cell: wall shear stress ( $\tau$ ) distribution;  $x$ , parallel to flow;  $y$ , perpendicular to flow.

The density of cells was adjusted  $3000 \text{ cells/cm}^2$  for seeding. Before each flow test, cells were cultured for 24 hours in the incubator without flow stimulation (without rotation of the disk) to make adhesion of cells to the bottom of the culture dish stable.

After the pre-incubation for 24 hours without shear, the cells were continuously sheared with the rotating disk for 24 hours in the incubator at the constant rotating speed. The value for the constant speed of the disk was preset for each test to adjust the shear stress field as the designed value.

### C. Migration Velocity and Area of Cell

During the cultivation of cell under the shear flow, the time-lapse microscopic images were taken every ten minutes. At each two-dimensional image, the contour of each cell adhered on the stationary plate of the scaffold was traced. The projected area ( $S$ ) at the image of each cell was calculated (Fig. 2). The area of each cell was traced before and after division: from  $S_1$  to  $S_2$  before division; from  $S'_1$  to  $S'_2$ , and from  $S''_1$  to  $S''_2$  after division, respectively. The contour of each cell was approximated to ellipsoid, and the centroid of each cell was used to track the migration of the cell (Fig. 3). The flow direction was defined as  $x$  axis. The direction to the rotating axis was defined as  $y$  axis, which is perpendicular to  $x$  axis. The components of the migration velocity were calculated as  $v_x$  and  $v_y$ . As  $y$  increases,  $r$  decreases. The shear stress ( $\tau$ ) decreases with  $y$  (1).

## III. RESULTS

Tracings of the area ( $S$ ) before and after division of each cell under the shear stress field of 1 Pa are displayed in Fig. 4 (L929) and Fig. 5 (3T3-L1). The time "zero" corresponds to the timing of division of the cell. The decrease of the area ( $S$ ) before division corresponds to the rounding of the cell before division. The markers of the same color show the same cell. After division, the markers of the same color correspond to cells divided from the same mother cell. After division, the area of each cell tends to return gradually to that of before division. The order of the size of cells after division tends to same as that before division.

The area of each cell before division is larger at L929 (Fig. 4) than at 3T3-L1 (Fig. 5). The area of each cell at division is around  $1000 \mu\text{m}^2$  regardless of the cell types. The decrease of the area of 3T3-L1 before division is slower than that of L929. The increase of the area of L929 after division is faster than that of 3T3-L1 in some cells.

The velocity of the migration of each cell under the shear stress field of 1 Pa is displayed at the  $x$ - $y$  plane in Figs. 6-9: L929 (Figs. 6 and 7), and 3T3-L1 (Figs. 8 and 9). The markers of data with the same color are correspond to classification by the term from the time of division of each cell: from  $-120$  min to  $-100$  min, from  $-100$  min to  $-80$  min, from  $-80$  min to  $-60$  min, from  $-60$  min to  $-40$  min, from  $-40$  min to  $-20$  min, and from  $-20$  min to  $0$  min before division; from  $0$  min to  $10$  min, from  $10$  min to  $20$  min, from  $20$  min to  $40$  min, from  $40$  min to  $60$  min, from  $60$  min to  $80$  min, from  $80$  min to  $100$  min, and  $100$  min to  $120$  min after division, respectively. In each  $x$ - $y$  plane, the distance from the origin of each datum point corresponds to the absolute value of the velocity of the cell. The datum point in the positive area of  $x$  corresponds to the migration to the downstream direction. The datum point in the negative area of  $x$  corresponds to the migration to the upstream direction. The datum point in the positive area of  $y$  corresponds to the migration to the rotating axis direction, where the shear stress is lower. The datum point in the negative area of  $y$  corresponds to the migration leaving from the rotating axis. The shear stress increases as the cell leaves from the rotating axis.

Concentrated distribution of data around the origin corresponds to the low velocities of cells. Several cells of L929 migrate to the direction perpendicular to the flow just before division (Fig. 6). Symmetric distribution of data shows the migration to random directions of L929 after division in Fig. 7. Some cells migrate with higher velocity to the direction of the rotating axis, where the wall shear stress is lower (Fig. 6). In some cells, the migration velocity is higher before division than after division. Quite a large number of cells migrate upstream (Fig. 7). The horizontal distribution of data shows that 3T3-L1 migrates parallel to the flow direction than the perpendicular direction (Figs. 8 and 9). Extended distribution to the positive  $x$  axis shows that cells tend to migrate downstream with the higher velocity (Figs. 8 and 9). Some cells migrate downstream with the higher velocity just after division (Fig. 9). Most of migration with the higher velocity occurred around the term of division of each cell.

The velocity components of  $v_x$  and  $v_y$  are plotted in relation to the area ( $S$ ) of each cell in Figs. 10-17. The markers of data with the same color are correspond to classification by the term from the time of division of each cell: from  $-120$  min to  $-100$  min, from  $-100$  min to  $-80$  min, from  $-80$  min to  $-60$  min, from  $-60$  min to  $-40$  min, from  $-40$  min to  $-20$  min, and from  $-20$  min to  $0$  min before division; from  $0$  min to  $10$  min, from  $10$  min to  $20$  min, from  $20$  min to  $40$  min, from  $40$  min to  $60$  min, from  $60$  min to  $80$  min, from  $80$  min to  $100$  min, and  $100$  min to  $120$  min after division. Data of L929 are displayed in Figs. 10-13. Data of 3T3-L1 are displayed in Figs. 14-17. Data before division are displayed in Figs. 10, 12, 14, and 16. Data after division are displayed in Figs. 11, 13, 15, and 17. Data of  $v_x$  are collected in Fig. 12, 13, 16, and 17. Data of  $v_y$  are collected in Fig. 10, 11, 14, and 15. The absolute value of the velocity of the cell migration tends to decrease with the increase of the area ( $S$ ) (Figs. 10, 11, 12, 13, 15, 16, and 17). The migration of each cell accelerates at the smaller contact area around the term of division of the cell. Some cells of L929 make migration with the higher velocity at the direction perpendicular to the flow (Figs. 10 and 11).

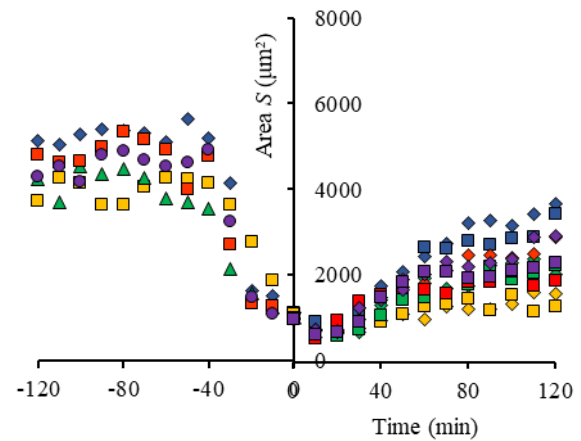


Fig. 4. Tracings of area ( $S$ ) at division of L929 under shear stress field of 1 Pa: before (left, minus), and after (right, plus). Same color shows tracings of each cell.

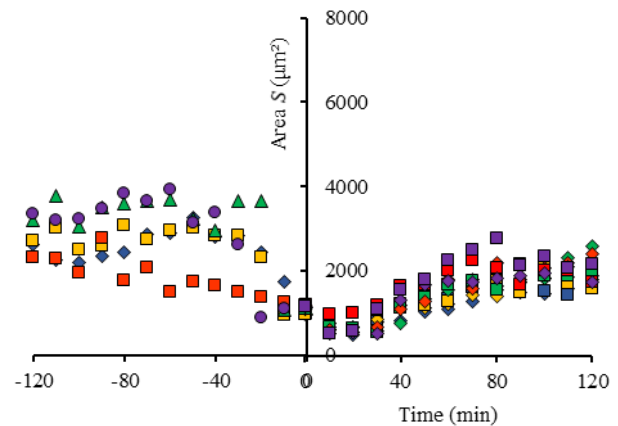


Fig. 5. Tracings of area ( $S$ ) at division of 3T3-L1 under shear stress field of 1 Pa: before (left, minus), and after (right, plus). Same color shows tracings of each cell.

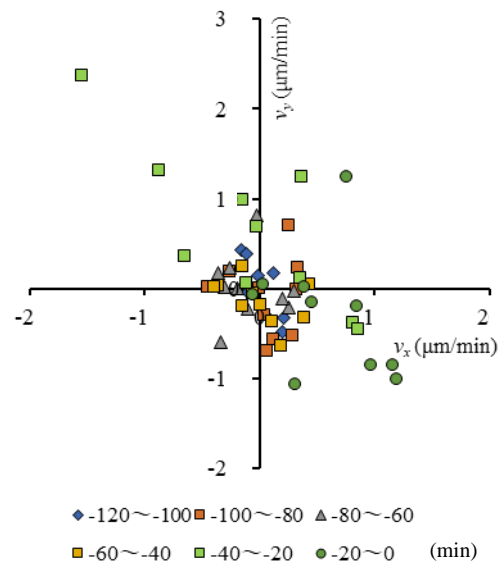
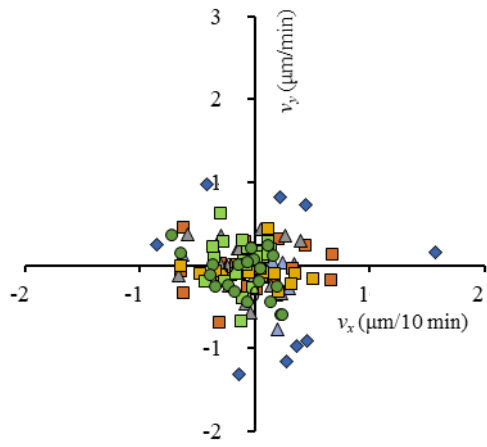
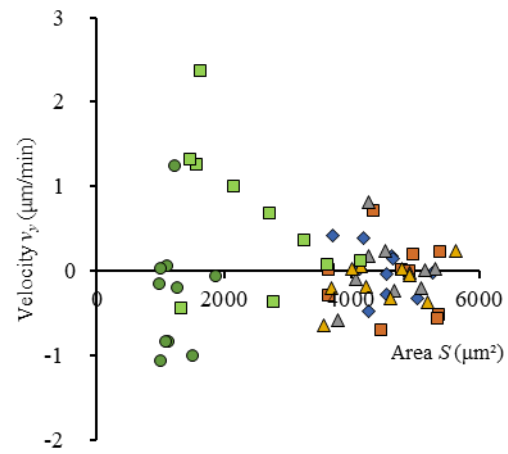


Fig. 6. Velocity of the migration ( $v_x$ ,  $v_y$ ) before division of L929 under shear stress field of 1 Pa.



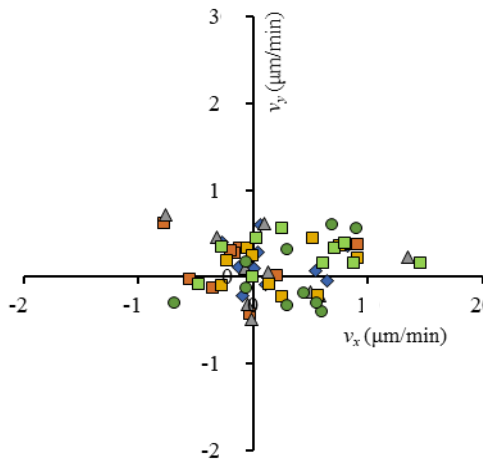
◆ 0~10    ▲ 10~20    ■ 20~40    ▲ 40~60  
 ■ 60~80    ■ 80~100    ● 100~120 (min)

Fig. 7. Velocity of the migration ( $v_x, v_y$ ) after division of L929 under shear stress field of 1 Pa.



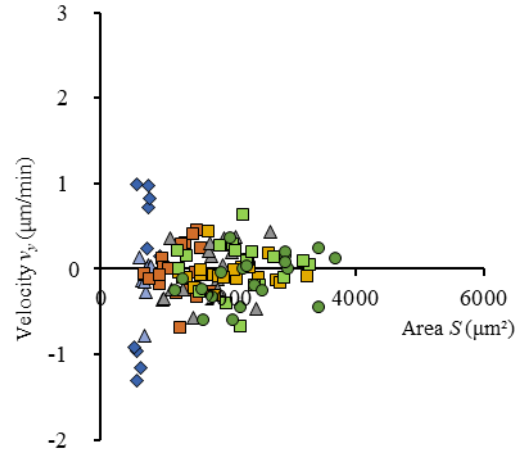
◆ -120~-100    ■ -100~-80    ▲ -80~-60  
 ▲ -60~-40    ■ -40~-20    ● -20~0 (min)

Fig. 10. Velocity of the migration  $v_y$  before division of L929 under shear stress field of 1 Pa in relation to area  $S$ .



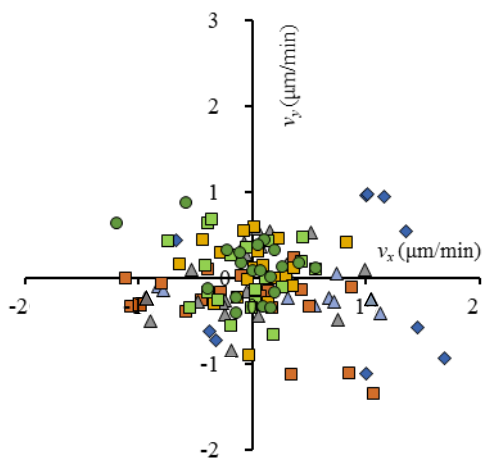
◆ -120~-100    ■ -100~-80    ▲ -80~-60  
 ■ -60~-40    ■ -40~-20    ● -20~0 (min)

Fig. 8. Velocity of the migration ( $v_x, v_y$ ) before division of 3T3-L1 under shear stress field of 1 Pa.



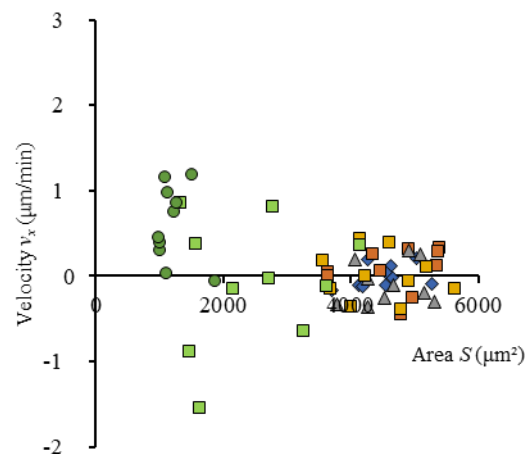
◆ 0~10    ▲ 10~20    ■ 20~40    ▲ 40~60  
 ■ 60~80    ■ 80~100    ● 100~120 (min)

Fig. 11. Velocity of the migration  $v_y$  after division of L929 under shear stress field of 1 Pa in relation to area  $S$ .



◆ 0~10    ▲ 10~20    ■ 20~40    ▲ 40~60  
 ■ 60~80    ■ 80~100    ● 100~120 (min)

Fig. 9. Velocity of the migration ( $v_x, v_y$ ) after division of 3T3-L1 under shear stress field of 1 Pa.



◆ -120~-100    ■ -100~-80    ▲ -80~-60  
 ■ -60~-40    ■ -40~-20    ● -20~0 (min)

Fig. 12. Velocity of the migration  $v_x$  before division of L929 under shear stress field of 1 Pa in relation to area  $S$ .

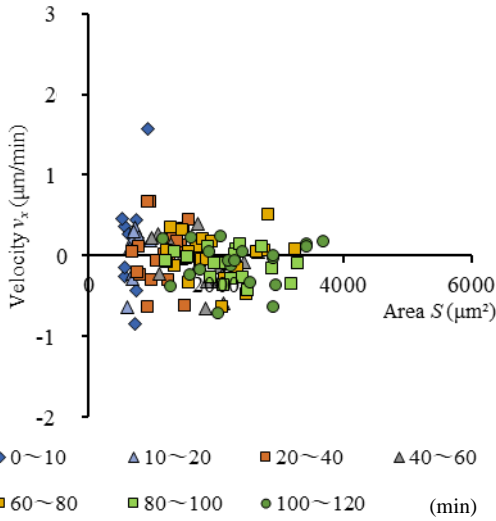


Fig. 13. Velocity of the migration  $v_x$  after division of L929 under shear stress field of 1 Pa in relation to area  $S$ .

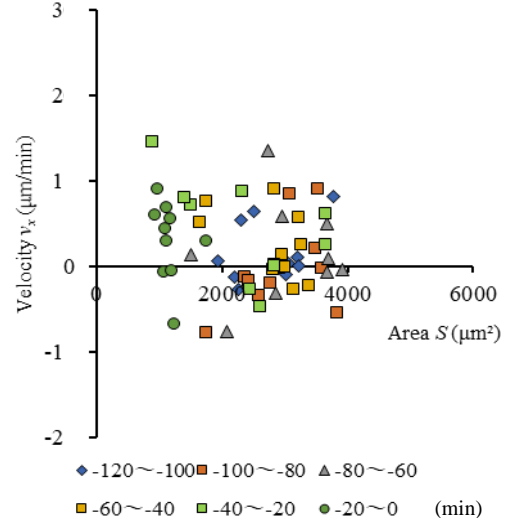


Fig. 16. Velocity of the migration  $v_x$  before division of 3T3-L1 under shear stress field of 1 Pa in relation to area  $S$ .

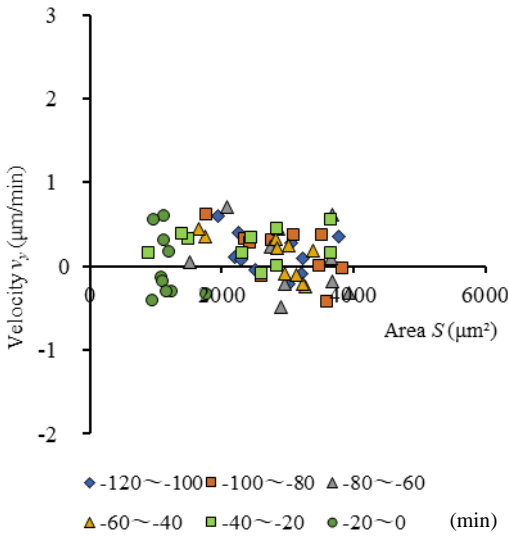


Fig. 14. Velocity of the migration  $v_y$  before division of 3T3-L1 under shear stress field of 1 Pa in relation to area  $S$ .

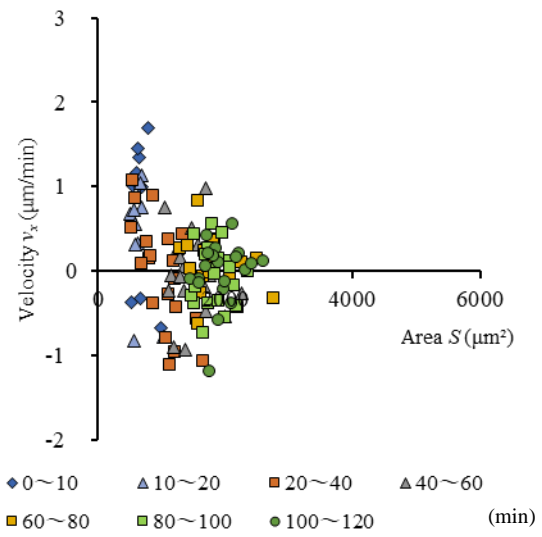


Fig. 17. Velocity of the migration  $v_x$  after division of 3T3-L1 under shear stress field of 1 Pa in relation to area  $S$ .

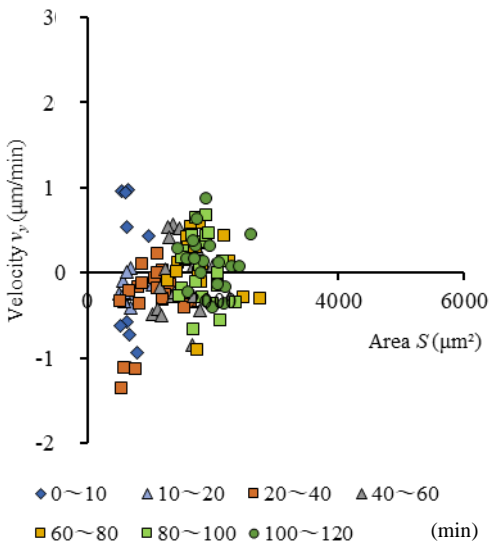


Fig. 15. Velocity of the migration  $v_y$  after division of 3T3-L1 under shear stress field of 1 Pa in relation to area  $S$ .

#### IV. DISCUSSION

Endothelial cells are exposed to the shear flow in the blood vessels *in vivo*. The effect of shear flow on endothelial cells was investigated in the previous studies [2–6]. Cells are exfoliated under the shear flow at the wall shear stress higher than 2 Pa [11]. A biological cell shows passive and active responses in an environment [1]. While the flow enhances the cell migration to the downstream, a cell migrates to adapt to the shear field. While the strong stimulation above the threshold damages the cell, the stimulation below the threshold remains in the cell as a memory for the response in the next step [13]. The hysteresis effect governs the active response of the cell.

In the previous study, cells were exposed to the shear flow in a donut-shaped open channel, and the effect of flow stimulation on cultured cells has been studied *in vitro* [7]. When the flow has an open surface, it is difficult to estimate the shear stress value in the fluid. Between two parallel walls, on the other hand, the parabolic velocity profile can be estimated in the laminar flow. In the previous studies, several

preparations were designed to study the effect of mechanical flow stimulations on biological cells: the tilting disk flow channel [11], the rhombus flow channel [14], the cross flow channel [15], and the rotating disk type [12].

The Couette type of flow is convenient to estimate the shear stress in the flow with the constant shear rate between the moving wall and the stationary wall, which is also available to non-Newtonian fluid. Several kinds of the devices of Couette type flow were designed for quantitative experiments of biological fluid in the previous studies [16, 17]. The cone-and-plate type device has the uniform shear field in the entire space between the rotating cone and the stationary plate [2, 3]. The shear stress is constant independent of the distance from the rotating axis. The erythrocyte destruction was studied between the rotating concave cone and the stationary convex cone [18].

A parallel disks system between rotating disk and the stationary disk, on the other hand, has several advantages: stability of the rotating motion of the disk, stability of the optical path for the microscopic observation, morphologic preciseness of the plane of the disks, and simultaneous observation over the range of variation of the shear rate proportional to the radius from the rotational axis [1]. In the radial direction, the field has the wall shear stress gradient. The shear stress gradients were also studied as the parameter which affects cells behavior [4, 6]. The floating erythrocyte deformation was observed between counter rotating parallel discs [19].

In the present study, the rotating parallel disk system is selected to make Couette type of flow instead of the cone and plate system. At the constant angular velocity of  $22 \text{ rad s}^{-1}$  ( $d = 0.3 \text{ mm}$ ), the shear rate ( $\dot{\gamma}$ ) increases from  $0.88 \times 10^3 \text{ s}^{-1}$  to  $1.3 \times 10^3 \text{ s}^{-1}$ , when the distance from the axis ( $r$ ) increases from  $0.012 \text{ m}$  to  $0.018 \text{ m}$  in the observation area (1). The range of the shear rate enables the simultaneous observation of the behavior of cells related to variation of the shear stress between  $1.3 \text{ Pa}$  and  $2.0 \text{ Pa}$  [12]. The rotating flow might induce the secondary flow by the centrifugal effect. The rotational speed of the disk is smaller than  $0.4 \text{ m s}^{-1}$  in the present system. The microscopic video image of the flowing cells between the rotating disk and the stationary disk shows the steady flow in the present experiment. Reynolds number ( $Re$ ) is calculated by (3).

$$Re = \rho v d / \eta = \rho r \omega d / \eta \quad (3)$$

In (3),  $\rho$  is density of the fluid,  $v$  is the circumferential velocity,  $\omega$  is the angular velocity,  $r$  is the distance from the rotating axis,  $d$  is the distance between the moving wall and the stationary wall, and  $\eta$  is the viscosity of the fluid.  $Re$  is  $1.5 \times 10^2$ , when  $\rho$ ,  $r$ ,  $\omega$ ,  $d$ , and  $\eta$  are  $1 \times 10^3 \text{ kg m}^{-3}$ ,  $0.018 \text{ m}$ ,  $22 \text{ rad s}^{-1}$ ,  $0.00056 \text{ m}$ , and  $0.0015 \text{ Pa s}$ , respectively. The turbulent flow may not occur in the flow of the small value of Reynolds number. The steady actual flow direction adjacent to the scaffold surface of cell culture has been confirmed by the streamline traced by the direction of exfoliation of the cell and of the moving particle adjacent to the surface [2]. The flow velocity, which increases in proportional to the distance from the rotating axis, has also been confirmed by tracings of the moving particle adjacent to the surface.

The most of myoblasts tend to migrate to the oblique direction of the lower shear stress field at  $1 \text{ Pa}$  [10]. The effect of shear flow on cells depends on the cell types. The dependency might be applied to the cell sorting technology [16]. After division, cells tend to migrate counter direction each other. The tendency makes symmetrical distribution of the migration velocity of cells in Fig. 7. Tracing of the cell after division is convenient to study on the initial behavior of the cell.

The cells proliferate regardless of the shear flow stimulation. The cell cycle does not vary under the shear flow [8]. The movement of each cell can be tracked by the time lapse image with the interval of ten minutes in the present experiment.

To evaluate the response depending on the cell type, comparison with the experimental results of more cell types is necessary [10]. A lot of supplementary works in molecular biology are necessary to analyze the mechanism of build-up tissue of oriented cells. More long term experiments are also necessary to trace the relation between the migration direction of the single cell and the orientation of cells in the tissue.

## V. CONCLUSION

The migration velocity of each single cell under the Couette type of the shear flow field has been studied in relation to the area adhere to the scaffold before and after division *in vitro*. The migration of each cell accelerates at the smaller contact area around the term of division of the cell. Several cells of L929 migrate to the direction perpendicular to the flow just before division. Although many cells migrate upstream, 3T3-L1 tends to migrate downstream.

## ACKNOWLEDGMENT

The authors thank to Mr. Hiromi Sugimoto and Mr. Kosuke Shimada for their assistance of the experiment.

## REFERENCES

- [1] S. Hashimoto, H. Sugimoto, and H. Hino, "Effect of couette type of shear stress field with axial shear slope on deformation and migration of cell: comparison between C2C12 and HUVEC," *Journal of Systemics Cybernetics and Informatics*, vol. 17, no. 2, 2019, pp. 4–10.
- [2] S. Hashimoto, H. Sugimoto, and H. Hino, "Behavior of cell in uniform shear flow field between rotating cone and stationary plate," *Journal of Systemics Cybernetics and Informatics*, vol. 16, no. 2, 2018, pp. 1–7.
- [3] M. H. Buschmann, P. Dieterich, N. A. Adams, and H. J. Schnittler, "Analysis of flow in a cone-and-plate apparatus with respect to spatial and temporal effects on endothelial cells," *Biotechnology and Bioengineering*, vol. 89, no. 55, 2005, pp. 493–502.
- [4] N. DePaola, M. A. Gimbrone Jr., P. F. Davies, and C. F. Dewey Jr., "Vascular endothelium responds to fluid shear stress gradients," *Arteriosclerosis Thrombosis and Vascular Biology*, vol. 12, no. 11, 1992, pp. 1254–1257.
- [5] M. A. Ostrowski, N. F. Huang, T. W. Walker, T. Verwijlen, C. Poplawski, A. S. Khoo, J. P. Cooke, G. G. Fuller, and A. R. Dunn, "Microvascular endothelial cells migrate upstream and align against the shear stress field created by impinging flow," *Biophysical Journal*, vol. 106, no. 2, 2014, pp. 366–374.
- [6] Y. Tardy, N. Resnick, T. Nagel, M. A. Gimbrone Jr., and C. F. Dewey Jr., "Shear stress gradients remodel endothelial monolayers *in vitro* via a cell proliferation-migration-loss cycle," *Arteriosclerosis Thrombosis and Vascular Biology*, vol. 17, no. 11, 1997, pp. 3102–3106.

- [7] S. Hashimoto, and M. Okada, "Orientation of cells cultured in vortex flow with swinging plate in vitro," *Journal of Systemics Cybernetics and Informatics*, vol. 9, no. 3, 2011, pp. 1–7.
- [8] Y. Endo, S. Hashimoto, and H. Eri, "Effect of shear stress on myoblasts cultured under couette type of shear flow between parallel disks," *Proc. 11th International Multi-Conference on Complexity Informatics and Cybernetics*, vol. 2, 2020, pp. 1–6.
- [9] Y. Endo, S. Hashimoto, and T. Tamura, "Effect of hysteresis of stimulation of tangential force field on alignment of 3T3-L1 cultured on micro striped pattern," *Proc. 11th International Multi-Conference on Complexity Informatics and Cybernetics*, vol. 2, 2020, pp. 7–12.
- [10] S. Hashimoto, K. Shimada, and Y. Endo, "Migration of cell under couette type shear flow field between parallel disks: after and before proliferation," *Proc. 11th International Multi-Conference on Complexity Informatics and Cybernetics*, vol. 2, 2020, pp. 19–24.
- [11] S. Hashimoto, F. Sato, H. Hino, H. Fujie, H. Iwata, and Y. Sakatani, "Responses of cells to flow in vitro," *Journal of Systemics Cybernetics and Informatics*, vol. 11, no. 5, 2013, pp. 20–27.
- [12] H. Hino, S. Hashimoto, Y. Takahashi, and M. Ochiai, "Effect of shear stress in flow on cultured cell: using rotating disk at microscope," *Journal of Systemics, Cybernetics and Informatics*, vol. 14, no. 4, 2016, pp. 6–12.
- [13] R. Steward Jr, D. Tambe, C. C. Hardin, R. Krishnan, and J. J. Fredberg, "Fluid shear, intercellular stress, and endothelial cell alignment," *American Journal of Physiology–Cell Physiology*, vol. 308, 2015, C657–C664.
- [14] F. Sato, S. Hashimoto, T. Yasuda, and H. Fujie, "Observation of biological cells in rhombus parallelepiped flow channel," *Proc. 17th World Multi-Conference on Systemics Cybernetics and Informatics*, vol. 1, 2013, pp. 25–30.
- [15] H. Hino, S. Hashimoto, Y. Takahashi, and S. Nakano, "Design of cross type of flow channel to control orientation of cell," *Proc. 20th World Multi-Conference on Systemics Cybernetics and Informatics*, vol. 2, 2016, pp. 117–122.
- [16] Y. S. Lin, W. Liu, and C. Hu, "Investigation of cells migration effects in microfluidic chips," *Journal of Chromatography Separation Techniques*, vol. 8, no. 1, 2017. P. 345.
- [17] S. Chung, R. Sudo, P. J. Mack, C. R. Wan, V. Vickerman, and R. D. Kamm, "Cell migration into scaffolds under co-culture conditions in a microfluidic platform," *Lab on a Chip*, vol. 9, no. 2, 2009, pp. 269–275.
- [18] S. Hashimoto, "Erythrocyte destruction under periodically fluctuating shear rate; comparative study with constant shear rate," *Artificial Organs*, vol. 13, no. 5, 1989, pp. 458–463.
- [19] S. Hashimoto, "Detect of sublethal damage with cyclic deformation of erythrocyte in shear flow," *Journal of Systemics Cybernetics and Informatics*, vol. 12, no. 3, 2014, pp. 41–46.